Loss of TSC complex enhances gluconeogenesis via upregulation of *Dlk1-Dio3* locus miRNAs

Dritan Liko[a], Andrzej Rzepiela[b], Vanja Vukojevic[c,d,e], Mihaela Zavolan[b] and Michael N. Hall[a*]

[a] Biozentrum, University of Basel CH-4056, Basel, Switzerland.
[b] Biozentrum, University of Basel and Swiss Institute of Bioinformatics, CH-4056, Basel, Switzerland.
[c] Division of Molecular Neuroscience, Department of Psychology, University of Basel, CH-4055, Basel, Switzerland.
[d] Transfaculty Research Platform Molecular and Cognitive Neurosciences, University of Basel, CH-4055, Basel, Switzerland.
[e] Department Biozentrum, Life Sciences Training Facility, University of Basel, CH-4056, Basel, Switzerland.

*Corresponding author: m.hall@unibas.ch

Classification
Biological Sciences; Cell Biology

Keywords
mTOR, miRNA, *Dlk1-Dio3*, glucose metabolism, CpG methylation

Author Contributions
D.L. and M.N.H. designed the research; D.L., A.R. and V.V. performed the research; M.Z. and M.N.H contributed resources and secured funding; D.L., A.R., V.V., M.Z. and M.N.H. analyzed the data; D.L. and M.N.H. wrote the paper.

This PDF file includes:
- Main Text
- Figures 1 to 5
- Supplemental Figures 1 to 4
- Supplemental Tables 1 to 3

Abstract

Loss of the tumor suppressor tuberous sclerosis complex 1 (*Tsc1*) in the liver promotes gluconeogenesis and glucose intolerance. We asked whether this could be attributed to aberrant expression of small RNAs. We performed small-RNA sequencing on liver of *Tsc1* knock-out mice, and found that miRNAs of the delta like homolog 1 (*Dlk1*) – deiodinase iodothyronine type III (*Dio3*) locus are upregulated in an mTORC1-dependent manner. Sustained mTORC1 signaling during development prevented CpG methylation and silencing of the *Dlk1-Dio3* locus, thereby increasing miRNA transcription. Deletion of miRNAs encoded by the *Dlk1-Dio3* locus reduced gluconeogenesis, glucose intolerance and fasting blood glucose levels. Thus, miRNAs contribute to the metabolic effects observed upon loss of TSC1 and hyperactivation of mTORC1 in the liver. Furthermore, we show that miRNA is a downstream effector of hyperactive mTORC1 signaling.

Significance

Organisms maintain a constant level of blood glucose. mTOR, an atypical serine/threonine kinase, plays a major role in glucose metabolism. This is evident in mouse models where disruption of mTOR signaling can cause a phenotype similar to a pre-diabetic state. However, how mTOR signaling affects blood glucose levels is incompletely understood. Here we show that sustained activation of mTORC1 enhances expression of miRNAs of the *Dlk1-Dio3* cluster to induce gluconeogenesis and increase blood glucose levels. Enhanced miRNA expression correlates to a reduction in levels of DNA methylation at the *Dlk1-Dio3* locus. Our findings reveal a connection between miRNAs, mTOR signaling and glucose metabolism, and may provide a new strategy in the treatment of metabolic disease.

Introduction

Mammalian Target of Rapamycin (mTOR) signaling integrates inputs from growth factors, nutrients and intracellular cues to regulate cell growth and metabolism (1, 2). mTOR forms two structurally and functionally distinct complexes, mTOR complex 1 (mTORC1) and mTORC2 (3, 4). Dysregulation of either complex can lead to metabolic disease and cancer (5, 6). A major negative regulator of mTORC1 is the tumor suppressor TSC complex that is composed of tuberous sclerosis 1 (TSC1), TSC2 and TBC1 domain family member 7 (TBC1D7) (7). Disruption of the TSC complex leads to increased mTORC1 signaling and disease (8, 9). There are a number of mouse models with aberrant mTOR signaling, virtually all of which exhibit dysregulation of glucose metabolism (10). Models in which mTOR signaling is upregulated develop tumors (10). For example, upregulation of mTORC1 signaling in mouse liver, achieved by deleting *Tsc1*, leads to impaired glucose homeostasis within weeks and to liver cancer within approximately 12 months (11-13).

The known effectors downstream of the mTOR complexes are proteins. Little is known about non-coding RNAs (ncRNAs), in particular microRNAs (miRNAs), that may mediate downstream effects of mTOR. miRNAs are a class of short non-coding RNAs involved in many aspects of cell growth and metabolism and, like mTOR, affect glucose metabolism and tumorigenesis (14). For example, dysregulation of a single miRNA, miR-122, in the liver affects liver metabolism and causes tumorigenesis (15, 16). miR-122 and other miRNAs are involved in liver development and homeostasis, and also in liver disease (17). Any given miRNA represses many targets and, as such, alterations in expression of one or a small number of miRNAs can impact many downstream processes (18). The coordinated control of many targets by a single miRNA is a means to mediate complex processes such as cellular metabolism.

miRNAs are encoded throughout the genome, including at imprinted loci from which expression is regulated by CpG methylation and heterochromatin maintenance in an allele-specific manner (19). The largest imprinted miRNA cluster is part of the *Dlk1-Dio3* locus, found in mouse chromosome 12. This is a nearly 1Mb imprinted locus that carries three paternally expressed protein-coding genes (*Dlk1*, retrotransposon-like protein 1 (*Rtl1*) and *Dio3*), and several maternally expressed non-coding genes. The latter include long non-coding RNA (lncRNA) genes, such as maternally expressed 3 (*Meg3*), *Anti-Rtl1*, RNA imprinted and accumulated in nucleus (*Rian*) and miRNA containing gene (*Mirg*), small nucleolar RNA (snoRNA) genes, Piwi-interacting RNA (piRNA) genes and more than 50 miRNA genes (20, 21). Like all imprinted loci, expression at the *Dlk1-Dio3* locus is controlled by CpG methylation of so-called imprinting control regions (ICRs). ICRs determine whether the paternal or maternal allele is expressed (21). The *Dlk1-Dio3* locus miRNAs, expressed from the maternal chromosome, are studied mainly in brain and placenta and are reported to be involved in metabolic disease and tumorigenesis (20, 22, 23).

It is well documented that miRNAs affect proteins involved in mTOR signaling (24, 25). However, only a few reports describe mTOR-mediated regulation of miRNA expression

(26-28). Moreover, to our knowledge, there is no evidence that mTOR signaling can affect specific miRNAs to control cellular metabolism. To determine whether miRNAs play a role in the metabolic alterations seen upon dysregulation of mTOR signaling, we examined miRNA expression in liver-specific *Tsc1* knock-out mice, hereafter referred as L-Tsc1KO mice. We report that upon loss of *Tsc1*, aberrantly constitutive mTORC1 signaling upregulates expression of miRNAs of the imprinted *Dlk1-Dio3* locus to enhance gluconeogenesis. These findings reveal a novel mode of mTORC1 signaling, showing that mTORC1 engages miRNAs to regulate metabolism.

Results

Non-coding RNAs of the Dlk1-Dio3 locus are up-regulated in L-Tsc1KO mouse liver. We utilized the L-Tsc1KO mouse model to investigate how miRNAs may contribute to the metabolic phenotypes observed upon constitutively high mTORC1 activity (*SI Appendix*, Fig. S1*A*). We performed small-RNA sequencing on livers of L-Tsc1KO animals and littermate controls, at 14 weeks of age when L-Tsc1KO mice display disrupted glucose metabolism but no sign of tumorigenesis. We found 31 and 6 miRNAs upregulated and downregulated, respectively, in L-Tsc1KO mice compared to controls (Fig. 1*A, SI Appendix*, Table S1). qPCR confirmed the changes in expression in all cases examined (Fig. 1*B*). 26 of the 31 upregulated miRNAs are encoded by the *Dlk1-Dio3* locus (*SI Appendix*, Table S1, miRNAs in bold).

DNA methylation at three distinct CpG regions, DLK1 differentially methylated region (DLK1-DMR), intergenic differentially methylated region (IG-DMR) and MEG differentially methylated region (MEG-DMR) controls expression of genes at the *Dlk1-Dio3* locus (29-31) (*SI Appendix,* Fig. S1*B*). The non-coding genes of the locus are expressed, from the maternal chromosome, as one transcript (21, 32, 33). Consistent with a single transcript, the *Meg3*, *Rian* and *Mirg* long non-coding RNAs were upregulated in L-Tsc1KO mice (Fig. 1*C*). Four other *Dlk1-Dio3* locus transcripts expressed from the maternal chromosome, the small nucleolar RNA MBII-343, the non-coding transcript ICR-ncRNA, and two pre-miRNAs were also upregulated (34) (Fig. 1*D*). In contrast, expression of the *Dlk1* and *Dio3* protein-coding genes did not change (Fig. 1*C* and *SI Appendix*, Fig. S1*C*). Thus, transcription of non-coding genes from the *Dlk1-Dio3* locus is up-regulated in the liver of L-Tsc1KO mice.

Up-regulation of Dlk1-Dio3 locus miRNAs is mTORC1 dependent. The miRNAs of the *Dlk1-Dio3* locus are expressed in pluripotent stem cells and in brain and placenta in adult mice (35). Furthermore, they are expressed in all tissues during embryogenesis and repressed after birth in liver and other tissues (36, 37). In contrast, we detected sustained expression of the miRNAs in L-Tsc1KO liver at 14 weeks of age. To determine whether the miRNAs are up-regulated throughout postnatal development, we measured hepatic expression of 3 *Dlk1-Dio3* miRNAs, at 2, 4 and 8 weeks of age. Mature miRNA levels were similar in control and L-Tsc1KO mice up to 4 weeks of age (*SI Appendix,* Fig. S2*A*). However, at 8 weeks, the

miRNAs were significantly more abundant in L-Tsc1KO mice (*SI Appendix,* Fig. S2*A*). This was due primarily to loss of miRNA expression in control littermates at 8 weeks, i.e., aberrantly sustained expression in the L-Tsc1KO mice (Fig. 2*A*). The L-Tsc1KO livers even exhibited a small increase in miRNA levels at 8 weeks compared to 4 weeks. (Fig. 2*A*). We further observed a clear downregulation of the three miRNAs at 8 weeks in pure C57BL/6J (wild type) mice compared to 4-week-old mice (Fig. 2*B*). These results demonstrate a physiological downregulation of *Dlk1-Dio3* locus miRNAs at 4 to 8 weeks of age. Furthermore, loss of *Tsc1* prevents this downregulation.

To determine if high mTORC1 activity in L-Tsc1KO mice is responsible for the observed dysregulation of *Dlk1-Dio3* locus miRNAs, we treated control and L-Tsc1KO mice with rapamycin, an allosteric mTORC1 inhibitor, or INK128, an mTOR kinase site inhibitor, from 4 to 8 weeks of age. Long term rapamycin and INK128 treatment partly reduced expression of the miRNAs at 8 weeks in L-Tsc1KO mice (Fig. 2*C* and *D*, *SI Appendix* Fig. S2*B* and *C*). INK128 also had a mild inhibitory effect on the already low levels of *Dlk1-Dio3* locus miRNAs in control mice at 8 weeks (Fig. 2*D*). Also, we note that mTOR signaling was not altered in untreated control mice at 4 and 8 weeks of age (*SI Appendix,* Fig. S2*D*). Thus, although the physiological inhibition of the *Dlk1-Dio3* locus miRNAs in wild type mice appears to be independent of mTOR signaling, elevated mTORC1 activity in L-Tsc1KO mice maintains hepatic expression of *Dlk1-Dio3* locus miRNA beyond 4 weeks of age.

To determine if the downregulation of miRNAs from 4 to 8 weeks is transcriptional, we assessed the hepatic levels of the lncRNAs of the *Dlk1-Dio3* locus at 4 and 8 weeks. Levels of *Meg3*, *Rian* and *Mirg* were comparable in 4-week-old control and L-Tsc1KO livers but significantly increased in 8-week-old L-Tsc1KO livers compared to controls (*SI Appendix*, Fig. S3*A* and *B*). Mirroring the level of miRNAs, the level of the lncRNAs was significantly reduced in control animals at 8 weeks when compared to 4-week-old mice. Moreover, 8-week-old L-Tsc1KO animals displayed a significant increase in levels of *Meg3*, *Rian* and *Mirg*, when compared to 4-week-old control or L-Tsc1KO livers (Fig. 2*E*). Similar to the miRNAs, long term rapamycin and INK-128 treatment prevented the high expression of *Meg3*, *Rian* and *Mirg* in L-Tsc1KO livers (Fig. 2*F* and *G*). Thus, constitutively high mTORC1 signaling sustains expression of *Dlk1-Dio3* miRNAs and other non-coding RNAs beyond 4 weeks of age.

mTOR prevents CpG methylation at the MEG-DMR of the Dlk1-Dio3 locus. CpG methylation of the IG and MEG DMRs, that lie between the *Dlk1* and *Meg3* genes, controls expression of the entire *Dlk1-Dio3* locus (21, 38). Methylation at the IG-DMR is thought to determine imprinting of the locus, while methylation of MEG-DMR appears to play a secondary role in controlling expression (39, 40). Bisulfite pyrosequencing revealed that CpG methylation at IG-DMR and MEG-DMR was significantly increased in control mice at 8 weeks of age compared to 4 weeks (Fig. 3*A*), which likely explains the reduced expression of miRNAs and other ncRNAs of the *Dlk1-Dio3* locus. Interestingly, L-Tsc1KO livers at 8 weeks of age showed significantly reduced CpG methylation of MEG-DMR but not of IG-DMR, compared to

controls (Fig. 3*A* and *SI Appendix*, Fig. S3*C*). Both DMRs exhibited similar CpG methylation levels in L-Tsc1KO and control samples at 4 weeks of age (*SI Appendix*, Fig. S3*C*). To confirm the methylation results obtained by bisulfite pyrosequencing, we assessed methylation changes using an assay based on cleavage by the HpaII and MsaI restriction enzymes, hereafter referred to as the restriction assay. We measured CpG methylation at sites adjacent to IG-DMR and MEG-DMR, as described in materials and methods section. Similar to the pyrosequencing results, the restriction assay showed an increase in CpG methylation at both DMRs in 8-week-old pure C57BL/6J (wild type) mice as compared to 4-week-old animals (Fig. 3*B*). As before, CpG methylation was reduced only at the MEG-DMR in 8-week-old L-Tsc1KO mouse livers compared to controls (Fig. 3*C* and *D*).

Next, we used the two methylation assays to determine the CpG methylation status of the MEG-DMR upon long term rapamycin or INK-128 treatment. Treatment was started at 4 weeks of age and the livers were examined at 8 weeks. The restriction assay revealed that rapamycin treated L-Tsc1KO animals showed an increase in CpG methylation at MEG-DMR as compared to vehicle treated controls (Fig. 3*E*). INK-128 treatment had a more pronounced effect in preventing loss of MEG-DMR methylation in L-Tsc1KO liver compared to controls (Fig. 3*F* and *G*). The partially increased CpG methylation in drug treated 8-week-old livers suggests that constitutively high mTORC1 signaling in L-Tsc1KO mice prevents CpG methylation of MEG-DMR and thereby sustains miRNA expression.

As the level of *Dlk1-Dio3* locus miRNAs was sustained in L-Tsc1KO animals even at 14 weeks of age, we assessed the CpG methylation of MEG-DMR at this timepoint. L-Tsc1KO mice exhibited reduced CpG methylation at MEG-DMR at 14 weeks of age, as observed at 8 weeks, compared to controls (Fig. 3*H*). Thus, the failure to CpG methylate MEG-DMR is also observed in older mice.

Methylation at many imprinted sites, including the *Dlk1-Dio3* locus, is maintained by the zinc finger protein 57 (ZFP57) – KRAB associated protein 1 (KAP1) – SET domain bifurcated 1 (SETDB1) complex. This complex recruits DNA methyl transferases (DNMTs) for de novo methylation, maintains already methylated CpG sites, and recruits other chromatin remodelers, such as nucleosome remodeling histone deacetylase (NURD) complex and heterochromatin protein 1 (HP1), to maintain a repressive chromatin environment (41, 42). Chromatin immunoprecipitation revealed decreased occupancy of KAP1 and SETDB1 at MEG-DMR in L-Tsc1KO liver (Fig. 3*I*, *SI Appendix* Fig. S3*D* and *E*). As the ZFP57-KAP1-SETDB1 complex maintains heterochromatin at CpG sites, we assessed histone occupancy at MEG-DMR in L-Tsc1KO liver at 14 weeks. We observed a reduction in overall histone occupancy in L-Tsc1KO liver, compared to controls (Fig. 3*J, SI Appendix* Fig. S3*F*). These findings suggest that the reduced presence of the ZFP57-KAP1-SETDB1 complex at MEG-DMR accounts for the decreased methylation at the *Dlk1-Dio3* locus in L-Tsc1KO liver.

Taken together, the above experiments support a model where aberrantly sustained mTORC1 activity disrupts CpG methylation and heterochromatin silencing of the *Dlk1-Dio3* locus that occurs starting at 4 weeks of age. Lack of both CpG methylation and heterochromatin silencing in L-Tsc1KO livers is maintained as mice age and contributes to

the continuous expression of the non-coding genes from the *Dlk1-Dio3* locus. Our findings also suggest that MEG-DMR, rather than IG-DMR, is the main site mediating transcriptional repression of non-coding genes. Constitutively high mTORC1 activity prevents CpG methylation and heterochromatin silencing at MEG-DMR, resulting in sustained expression of miRNAs and the lncRNAs of the *Dlk1-Dio3* locus.

Aberrant expression of Dlk1-Dio3 miRNAs causes metabolic defects. L-Tsc1KO mice exhibit increased gluconeogenesis and glucose intolerance (10, 43, 44). To determine if this phenotype is due to aberrantly high expression of *Dlk1-Dio3* miRNAs, we introduced a deletion of the so-called miR-379/miR-410 region of the *Dlk1-Dio3* locus into the L-Tsc1KO mouse (*SI Appendix*, Fig. S4*A*). The miR-379/miR-410 region includes 41 miRNA genes of the *Dlk1-Dio3* locus. We note that this deletion does not change mTORC1 signaling (*SI Appendix*, Fig. S4*B*). As shown previously, full body deletion of the miR-379/miR-410 region, hereafter referred to as miRKO , causes partial (30%) litter mortality upon weaning due to a defect in glucose metabolism, in particular low blood glucose (45). Like miRKO mice, L-Tsc1KO miRKO mice displayed partial litter mortality and no obvious phenotype as adults. We performed glucose tolerance tests (GTT) and pyruvate tolerance tests (PTT) on control, L-Tsc1KO, miRKO and L-Tsc1KO miRKO mice. L-Tsc1KO mice exhibited glucose intolerance and increased gluconeogenesis, whereas miRKO mice displayed neither, as compared to control mice (Fig. 4*A* and *B*, *SI Appendix* Fig. S4*C* and *D*). Interestingly, L-Tsc1KO miRKO mice showed improved glucose tolerance and reduced gluconeogenesis compared to L-Tsc1KO mice (Fig. 4*C* and *D*). These observations suggest that aberrantly increased levels of the *Dlk1-Dio3* locus miRNAs play a role in the metabolic phenotype of L-Tsc1KO mice.

Glucose-6-phosphatase (G6P), fructose-1,6-bisphosphatase (FBP), phospho-enol-pyruvate carboxykinase (PEPCK) and pyruvate carboxylase (PC) are enzymes that catalyze gluconeogenesis. The genes expressing these enzymes were upregulated in L-Tsc1KO mice, as compared to control mice, and reduced in L-Tsc1KO miRKO mice, as compared to L-Tsc1KO mice (Fig. 4*E* and *F*). Further, rapamycin treatment showed a trend in downregulation of expression of the gluconeogenetic genes (*SI Appendix* Fig. S4*E)* in a manner, as shown above, that correlates with decreased levels of *Dlk1-Dio3* locus miRNAs, in L-Tsc1KO mice. It was previously shown that the increased rate of gluconeogenesis in L-Tsc1KO mice, compared to wild type controls, is due to reduced Protein Kinase B (PKB, also known as AKT) signaling that in turn leads to de-repression of the Forkhead Box Protein (FOXO) transcription factors (11, 44). We did not see a significant difference in phosphorylation of AKT and FOXO in L-Tsc1KO liver compared to L-Tsc1KO miRKO liver (*SI Appendix* Fig. S4*F*). Thus, *Dlk1-Dio3* miRNAs promote gluconeogenesis via transcriptional activation of gluconeogenic genes and this effect is independent of the AKT-FOXO axis.

Gluconeogenesis is turned on during periods of fasting to maintain blood glucose levels. After 18 hours of fasting, blood glucose levels in L-Tsc1KO mice were high compared to controls (Fig. 4*G*). Interestingly, the increased fasting blood glucose levels were normalized in L-Tsc1KO miRKO mice as compared to L-Tsc1KO mice (Fig. 4*H*). These results

suggest that miRNAs of the *Dlk1-Dio3* locus, in particular the miRNAs in the miR-379/miR-410 region, maintain blood glucose levels during fasting. Taken together, our findings suggest that pathologically high mTOR signaling induces expression of miRNAs to promote gluconeogenesis. Furthermore, we propose that high mTORC1 signaling induces miRNA expression most likely by preventing CpG methylation of the *Dlk1-Dio3* locus (Fig. 5).

Discussion

Here we show that constitutively high mTORC1 signaling, due to loss of the tumor suppressor *Tsc1*, up-regulates miRNAs of the *Dlk1-Dio3* locus to possibly increase gluconeogenesis. Furthermore, we report that the developmentally expressed miRNAs of the *Dlk1-Dio3* locus are transcriptionally silenced in the liver of wild type mice at 4 to 8 weeks of age, but remain expressed in L-Tsc1KO livers. Sustained expression of the *Dlk1-Dio3* locus miRNAs, upon high mTOR activity, correlated with lower CpG methylation of the *Dlk1-Dio3* locus.

How does pathologically high mTORC1 activity (loss of *Tsc1*) prevent CpG methylation of the *Dlk1-Dio3* locus to maintain expression of miRNAs? In wild type mouse livers, we observed more CpG methylation at IG-DMR and MEG-DMR of the *Dlk1-Dio3* locus at 8 weeks of age, compared to 4 weeks. Loss of *Tsc1* prevented CpG methylation at MEG-DMR but not at IG-DMR. The interplay between IG-DMR and MEG-DMR CpG methylation and downstream consequences are still being unraveled (29, 46-48), but our data suggest that methylation at the IG- and MEG-DMRs are independently controlled. TSC1 appears to promote methylation at MEG-DMR without affecting methylation at IG-DMR. How loss of TSC1 prevents CpG methylation at MEG-DMR is unclear. CpG methylation is maintained by the ZFP57-KAP1-SETDB1 complex. We observed reduced histone and ZFP57-KAP1-SETDB1 complex occupancy at MEG-DMR upon loss of TSC1. The reduced binding by the complex could lead to decreased recruitment of the histone depositing enzyme HP1 which would in turn account for less histones and increased miRNA expression. mTORC1 may phosphorylate members of the ZFP57-KAP1-SETDB1 complex, accounting for the increase in miRNA expression upon loss of TSC1. Interestingly, KAP1 was detected as a potential mTOR substrate in large scale screens (49-51). Alternatively, mTORC1 may phosphorylate a factor directly involved in transcription of *Dlk1-Dio3* locus miRNAs. Sustained mTOR activity may promote recruitment of this factor to MEG-DMR, thereby preventing methylation of the site. Proteins such as DPPA3, AFF3 or CTCF have been shown to act at the MEG-DMR (52-55). It would be interesting to determine if they are targets of mTOR.

How do the miRNAs of the *Dlk1-Dio3* locus activate gluconeogenesis? Upon deletion of the miR-379/miR-410 region in L-Tsc1KO mice, we observed reduced transcription of gluconeogenic genes. It is possible that *Dlk1-Dio3* locus miRNAs promote gluconeogenesis by inhibiting one or more negative regulators of gluconeogenic enzymes. AKT negatively regulates gluconeogenic genes by phosphorylating and inhibiting FOXO transcription factors. Loss of TSC1 reduces, via a negative feedback loop, AKT activity but deletion of the miR-379/miR-410 region in the L-Tsc1KO background did not restore phosphorylation of

AKT and FOXO. Thus, the effect of *Dlk1-Dio3* locus miRNAs on gluconeogenesis appears to be independent or downstream of the AKT-FOXO axis. Also, gluconeogenic flux is controlled post-transcriptionally via increased levels of AMP and/or changes in the NAD^+/NADH ratio (56-59). It is possible that increased expression of *Dlk1-Dio3* locus miRNAs alters the level of AMP and/or NAD^+/NADH ratio which may in turn affect gluconeogenesis. It remains to be determined how up-regulation or deletion of the *Dlk1-Dio3* locus affects gluconeogenesis and fasting blood glucose levels. We also note that the miR-379/miR-410 region of the *Dlk1-Dio3* locus is deleted in the entire body and, as such, the phenotype seen with the L-Tsc1KO miRKO mice could potentially originate outside of the liver.

Our findings add a new dimension to mTOR signaling and how it affects glucose metabolism. To our knowledge, this is the first report showing that mTORC1 signals through miRNA, and does so to impact glucose metabolism. Sustained expression of *Dlk1-Dio3* locus miRNAs can explain the pathological increase in gluconeogenesis and blood glucose levels upon loss of TSC1. *Dlk1-Dio3* locus miRNAs may be necessary to maintain elevated glucose levels in blood and tissues during mouse embryogenesis and periods of lactation. However, in adult mice, aberrantly increased levels of these miRNAs may cause high blood glucose levels that can produce a pre-diabetic phenotype. The *Dlk1-Dio3* locus found in mouse chromosome 12, is conserved in humans in chromosome 14 and is linked to disease upon dysregulation. Consistent with our findings, patients with Temple Syndrome, characterized with increased expression of *Dlk1-Dio3* locus miRNAs, are obese and may develop diabetes (60, 61). The targets of *Dlk1-Dio3* locus miRNAs and how they affect gluconeogenesis remain to be identified.

Materials and Methods

RNA isolation

Total RNA was isolated from 50mg of mouse liver and was homogenized in 1ml TRIzol (Sigma) using lysing matrix D tubes (Q-Biogene) and a bead beater. Subsequent steps were performed as per TRIzol manufacturer's instructions.

Small RNA sequencing and analysis

Total RNA was isolated as described above and 1ug of total RNA was used to generate small RNA libraries for sequencing as described in (62). Libraries were sequenced on an Illumina HiSeq-2500 deep sequencer. For analysis, the raw miRNA sequencing data was uploaded to the ClipZ server (63) for adapter removal and annotation. Differentially expressed miRNAs were extracted using DESeq (64) implemented as a Bioconductor package. A cutoff at 0.05 for the adjusted p-value provided by DESeq was used to filter the hits.

Quantitative Reverse Transcriptase PCR

For mRNAs quantitative PCR was performed from 200ng of total RNA, isolated as described above. DNAse digestion was performed using the Roche RNAse free DNAse kit (Roche) as per manufacturer's instructions. cDNA synthesis was performed using iScript (Bio-RAD) as per manufacturer's instructions. Samples were diluted 10 times prior to usage as a template in qPCR reactions together with SYBR Green Mix (Applied Biosystems) and primers. An Applied Biosystems StepOnePlus Real-Time PCR System was used. Relative expression levels were determined by normalizing each CT value to TBP expression using the $\Delta\Delta$CT method. Sequences of the primers used are in supplemental table 3.

For miRNAs quantitative PCR was performed from 2pg of total RNA that was used as a template together with the Applied Biosystems miRNA kit (Applied Biosystems) as per manufacturer's instructions to generate cDNA. miRNA Taqman primers from Invitrogen for miR-127, miR-34a, miR-376b, miR-381, miR-455, miR-541 and miR-802 (Cat #4427975) were used to perform the PCR reaction together with Taqman Universal 2X mastermix (Applied Biosystems) as per manufacturer's instructions. An Applied Biosystems StepOnePlus Real-Time PCR Systems was used. Relative expression levels were determined by normalizing each CT value to U6 expression using the $\Delta\Delta$CT method. Sequences of other primers used are shown in supplemental table 3.

Protein isolation and western blotting

Livers from mice were rapidly dissected and flash frozen in liquid nitrogen. For protein extraction liver tissues were homogenized using Polytron machine (Polytron) in ice-cold T-PER lysis buffer (Invitrogen) supplemented with protease and phosphatase inhibitors (Sigma). Lysates were cleared by centrifugation at 10,000xg for 15 minutes at 4^0C. Total protein concentration was assessed using a BCA Protein Assay kit (Invitrogen) as per

manufacturer's instructions. 10ug of protein was loaded on a gradient SDS/PAGE gel and transferred to a nitrocellulose membrane for blotting. Antibodies used are shown in supplemental table 2. Samples were probed overnight with primary antibody and 1 hour with secondary antibody conjugated to HRP. Supersignal West Pico chemiluminescent kit (Thermo Fischer) was used to detect staining in a Fusion X machine (Vilber).

Rapamycin and INK128 treatments

For chronic mTOR inhibition 4-week-old mice were injected intraperitoneally daily for 4 weeks with Rapamycin at 1mg/kg or INK128 at 0.5mg/kg or the respective vehicle. Rapamycin was dissolved in 5% PEG-400, 4% Ethanol and 5% Tween 80. INK128 was dissolved in 5% 1-methyl-2-pyrrolidinone, 15% polyvinylpyrrolidone K30 and 80% water. In all cases the injection volume did not supersede 100ul.

Statistical analysis

Unless stated otherwise, statistical significance was measured using a Student's unpaired *t* test to determine differences among groups. The differences were considered to be significant if $p < 0.05$. Data are presented as mean ± SEM. The asterisks represent the degree of significance: * $p<0.05$; ** $p<0.01$, *** $p<0.001$.

Glucose, and Pyruvate Tolerance Tests

For glucose tolerance tests (GTT) mice were fasted for 18 hours and administered 2g/kg of body weight glucose by intraperitoneal injection (i.p.). Blood glucose levels were measured in 10-minute intervals for 180 minutes. For pyruvate tolerance tests (PTT) mice were fasted for 18 hours before administering 2g/kg of body weight sodium pyruvate via i.p. injection. Blood glucose levels were measured in 10-minute intervals for a duration of 150 minutes. For each test at least 6 male mice of 14 to 16 weeks of age per condition were used.

Mouse Husbandry

L-Tsc1KO mice and miRKO mice were generated as described previously (45, 50). L-Tsc1KO miRKO mice were generated during this work by crossing L-Tsc1KO mice to miRKO mice. Littermate controls were used in all experiments. To determine the genotype PCR was done as described previously (45, 65). Mice were maintained under temperature and humidity-controlled conditions with 12-hour light and 12-hour dark cycle with free access to food and water. All experiments were performed in accordance with federal guidelines and were approved by the Kantonales Veterinaeramt of Kanton Basel-Stadt.

Pyrosequencing analysis

Tissues were ground in dry ice and DNA was isolated using DNA blood and tissue kit (Qiagen) as per manufacturer's instructions. Five-hundred nanograms of high-purity, intact DNA was used for bisulfite conversion using an EZ DNA Methylation-Gold kit (Zymo Research) by following standard protocols. Bisulfite converted (BSC) DNA quality and

concentration was determined using an RNA Pico 6000 Kit on a Bioanalyzer 2100 instrument (Agilent Technologies, USA) and Nanodrop 2000 (ThermoScientific). Bisulfite-converted (BSC) samples were normalized to 10 ng/µl. Primers were designed according to recommendations of (66): IG-DMR_5prime FW-5'-GTGGTTTGTTATGGGTAAGTTT-3' and RV-5'(Btn)- CCCTTCCCTCACTCCAAAAATTA-3'; MEG-DMR_5prime FW-5'-AGTTTGGGATTTAAAATTAAGGTTT-3' and RV-5'(Btn)-CTAAAAACTATCACCCCCACAT-3' (Microsynth). Promoter fragments were amplified using an AmplyTaq Gold Kit from Applied Biosystems (Life Technologies). PCR was done in 30 µl reactions containing the following: 1x PCR buffer II, 300 µM deoxynucleotide triphosphates, final 3.5 mM MgCl2, 200 µM of each primer, 20 ng of BSC DNA. We used the following cycling conditions: 95°C, 15 min–50 x (95°C, 30 s; 55°C, 30 s; 72°C, 30 s)–72°C, 10 min. PCR products were purified and sequenced using a PyroMark ID System (Biotage) following the manufacturer's suggested protocol and sequencing primers: for IG-DMR_5prime 5'- GTTTTATGGTTTATTGTATATAATG-3'; for MEG-DMR_5prime 5'- TTTTTGTTTTAATAATGTTAAATTT-3' (Microsynth). Controlling for PCR temperature bias was done with a series of calibrator samples of known methylation levels. Briefly, unmethylated standards were prepared by using two rounds of linear whole-genome amplification with an Ovation WGA System Kit (Nugene), starting from 10 ng of DNA, as recommended by the manufacturer. Methylated standards were made using CpG methyltransferase assay with *M.SssI* (New England Biolabs, USA) starting from 2 µg of purified DNA, following the standard protocol. Bisulfite conversion of standard samples was done as described above. All samples were analyzed in quadruplicates. Differential methylation analysis was performed using linear models, limma R package, multiple linear regression was used to determine significance (67). DNA methylation levels were averaged across CpGs in the examined promoter regions. To account for multiple testing, we applied Bonferroni correction.

Restriction Assay

DNA from tissues was isolated using DNA blood and tissue kit (Qiagen) as per manufacturer's instructions. Restriction Assays were performed using the EpiJet 5-mC analysis kit (Thermo Scientific) as per manufacturer's instructions. The following primers were used to check for the methyl-C at the IG-DMR and MEG-DMR. For IG-DMR 5'-CTGCAGCCGCTATGCTATG-3' and 5'- CAGCTAACCTGAGCTCCATG-3'. For MEG-DMR 5'-GACGAAGAGCTGGAATAGAG-3' and 5'-CATGTCCAGGAGGACGGAG-3'

Measuring Fasting Blood Glucose Levels

In order to measure the fasting blood glucose levels mice were starved for 18 hours a minimal amount of tail skin was cut and an Aviva glucometer device (Accu-check) was used to measure the concentration of glucose in a drop of blood. For each test at least 6 male mice of 14 to 16 weeks of age were used.

Chromatin Immunoprecipitation

Mouse livers were homogenized in cold PBS solution and crosslinked with 1% formaldehyde for 15 min at room temperature. Crosslinking was stopped with 0.125M glycine and homogenates were centrifuged at 600xg for 15 minutes. The cell pellets were resuspended in lysis buffer (5mM Pipes, 85mM KCl, 0.5% Nonidet P-40) supplemented with protease inhibitors (Roche) and incubated at room temperature for 30 min. Cell lysates were centrifuged at 5000xg for 15 minutes and nuclei were resuspended in nuclei lysis buffer (50mM Tris-HCl, 10mM EDTA, 1% SDS) for 30 minutes in room temperature. Chromatin was sonicated three times for 15 seconds using a Branson probe sonicator at 80% power setting. 50ug of DNA was incubated with 1ug of antibody in the cold room overnight and further incubated with a mix of A/G beads (Pierce) for 2 hours. Beads were washed three times in the cold room as per manufacturer's instruction and eluted with 0.1M NaHCO3, 1% SDS buffer. Crosslinking was reversed by incubation at 65^0C for 6 hours. DNA was purified using phenol chloroform-isoamyl alcohol (25:24:1) extraction and ethanol precipitated. Recovered DNA was used in qPCR reactions and data is expressed as percentage of the input. Antibodies used are shown in supplemental table 2 and primers used to amplify the DNA are 5'- GACGAAGAGCTGGAATAGAG-3' and 5'- CATGTCCAGGAGGACGGAG-3' for MEG-DMR, for the transcribed region primers that map at GAPDH, (Active Motif 71016) , were used, and for the non-transcribed region primers that map to a gene desert (Active Motif 71011) , were used.

Data Availability

Small-RNA sequencing data have been deposited in the Gene Expression Omnibus (GEO) database, https://www.ncbi.nlm.nih.gov/geo, (accession no. will be provided during proofs).

Acknowledgments

We thank Jerome Cavaille and Virginie Marty for providing the miR-379/miR-410 knock-out mouse. This work was supported by the Swiss National Science Foundation, NCCR RNA and Disease, ERC (MERiC), and the Louis-Jeantet Foundation.

References

1. M. Laplante, D. M. Sabatini, mTOR signaling in growth control and disease. *Cell* **149**, 274-293 (2012).
2. M. Shimobayashi, M. N. Hall, Making new contacts: the mTOR network in metabolism and signalling crosstalk. *Nat Rev Mol Cell Biol* **15**, 155-162 (2014).
3. R. Loewith *et al.*, Two TOR complexes, only one of which is rapamycin sensitive, have distinct roles in cell growth control. *Mol Cell* **10**, 457-468 (2002).
4. S. Wullschleger, R. Loewith, M. N. Hall, TOR signaling in growth and metabolism. *Cell* **124**, 471-484 (2006).
5. D. Liko, M. N. Hall, mTOR in health and in sickness. *J Mol Med (Berl)* **93**, 1061-1073 (2015).
6. R. A. Saxton, D. M. Sabatini, mTOR Signaling in Growth, Metabolism, and Disease. *Cell* **168**, 960-976 (2017).
7. C. C. Dibble *et al.*, TBC1D7 is a third subunit of the TSC1-TSC2 complex upstream of mTORC1. *Mol Cell* **47**, 535-546 (2012).
8. K. Inoki, Y. Li, T. Zhu, J. Wu, K. L. Guan, TSC2 is phosphorylated and inhibited by Akt and suppresses mTOR signalling. *Nat Cell Biol* **4**, 648-657 (2002).
9. B. D. Manning, A. R. Tee, M. N. Logsdon, J. Blenis, L. C. Cantley, Identification of the tuberous sclerosis complex-2 tumor suppressor gene product tuberin as a target of the phosphoinositide 3-kinase/akt pathway. *Mol Cell* **10**, 151-162 (2002).
10. V. Albert, M. N. Hall, mTOR signaling in cellular and organismal energetics. *Curr Opin Cell Biol* **33C**, 55-66 (2014).
11. H. L. Kenerson, M. M. Yeh, R. S. Yeung, Tuberous sclerosis complex-1 deficiency attenuates diet-induced hepatic lipid accumulation. *PLoS One* **6**, e18075 (2011).
12. S. Menon *et al.*, Chronic activation of mTOR complex 1 is sufficient to cause hepatocellular carcinoma in mice. *Sci Signal* **5**, ra24 (2012).
13. S. Sengupta, T. R. Peterson, M. Laplante, S. Oh, D. M. Sabatini, mTORC1 controls fasting-induced ketogenesis and its modulation by ageing. *Nature* **468**, 1100-1104 (2010).
14. D. P. Bartel, Metazoan MicroRNAs. *Cell* **173**, 20-51 (2018).
15. J. Burchard *et al.*, microRNA-122 as a regulator of mitochondrial metabolic gene network in hepatocellular carcinoma. *Mol Syst Biol* **6**, 402 (2010).
16. C. Jopling, Liver-specific microRNA-122: Biogenesis and function. *RNA Biol* **9**, 137-142 (2012).
17. Y. Chen, C. M. Verfaillie, MicroRNAs: the fine modulators of liver development and function. *Liver Int* **34**, 976-990 (2014).
18. J. Hausser, M. Zavolan, Identification and consequences of miRNA-target interactions--beyond repression of gene expression. *Nat Rev Genet* **15**, 599-612 (2014).
19. M. S. Bartolomei, A. C. Ferguson-Smith, Mammalian genomic imprinting. *Cold Spring Harb Perspect Biol* **3** (2011).
20. L. Benetatos *et al.*, The microRNAs within the DLK1-DIO3 genomic region: involvement in disease pathogenesis. *Cell Mol Life Sci* **70**, 795-814 (2013).
21. S. T. da Rocha, C. A. Edwards, M. Ito, T. Ogata, A. C. Ferguson-Smith, Genomic imprinting at the mammalian Dlk1-Dio3 domain. *Trends Genet* **24**, 306-316 (2008).

22. M. Lackinger *et al.*, A placental mammal-specific microRNA cluster acts as a natural brake for sociability in mice. *EMBO Rep* **20** (2019).
23. V. Marty *et al.*, Deletion of the miR-379/miR-410 gene cluster at the imprinted Dlk1-Dio3 locus enhances anxiety-related behaviour. *Hum Mol Genet* **25**, 728-739 (2016).
24. K. Tumaneng *et al.*, YAP mediates crosstalk between the Hippo and PI(3)K-TOR pathways by suppressing PTEN via miR-29. *Nat Cell Biol* **14**, 1322-1329 (2012).
25. H. Zhu *et al.*, The Lin28/let-7 axis regulates glucose metabolism. *Cell* **147**, 81-94 (2011).
26. B. Ogorek *et al.*, TSC2 regulates microRNA biogenesis via mTORC1 and GSK3beta. *Hum Mol Genet* **27**, 1654-1663 (2018).
27. M. J. Warner *et al.*, S6K2-mediated regulation of TRBP as a determinant of miRNA expression in human primary lymphatic endothelial cells. *Nucleic Acids Res* **44**, 9942-9955 (2016).
28. P. Ye *et al.*, An mTORC1-Mdm2-Drosha axis for miRNA biogenesis in response to glucose- and amino acid-deprivation. *Mol Cell* **57**, 708-720 (2015).
29. M. Kagami *et al.*, The IG-DMR and the MEG3-DMR at human chromosome 14q32.2: hierarchical interaction and distinct functional properties as imprinting control centers. *PLoS Genet* **6**, e1000992 (2010).
30. S. P. Lin *et al.*, Differential regulation of imprinting in the murine embryo and placenta by the Dlk1-Dio3 imprinting control region. *Development* **134**, 417-426 (2007).
31. S. Takada *et al.*, Epigenetic analysis of the Dlk1-Gtl2 imprinted domain on mouse chromosome 12: implications for imprinting control from comparison with Igf2-H19. *Hum Mol Genet* **11**, 77-86 (2002).
32. H. Seitz *et al.*, A large imprinted microRNA gene cluster at the mouse Dlk1-Gtl2 domain. *Genome Res* **14**, 1741-1748 (2004).
33. S. Tierling *et al.*, High-resolution map and imprinting analysis of the Gtl2-Dnchc1 domain on mouse chromosome 12. *Genomics* **87**, 225-235 (2006).
34. S. K. Kota *et al.*, ICR noncoding RNA expression controls imprinting and DNA replication at the Dlk1-Dio3 domain. *Dev Cell* **31**, 19-33 (2014).
35. L. Benetatos, G. Vartholomatos, E. Hatzimichael, DLK1-DIO3 imprinted cluster in induced pluripotency: landscape in the mist. *Cell Mol Life Sci* **71**, 4421-4430 (2014).
36. J. C. Kwekel *et al.*, Sex and age differences in the expression of liver microRNAs during the life span of F344 rats. *Biol Sex Differ* **8**, 6 (2017).
37. J. Schug *et al.*, Dynamic recruitment of microRNAs to their mRNA targets in the regenerating liver. *BMC Genomics* **14**, 264 (2013).
38. R. Benezra *et al.*, Id: a negative regulator of helix-loop-helix DNA binding proteins. Control of terminal myogenic differentiation. *Ann N Y Acad Sci* **599**, 1-11 (1990).
39. A. Gagne *et al.*, Analysis of DNA methylation acquisition at the imprinted Dlk1 locus reveals asymmetry at CpG dyads. *Epigenetics Chromatin* **7**, 9 (2014).
40. T. Saito, S. Hara, M. Tamano, H. Asahara, S. Takada, Deletion of conserved sequences in IG-DMR at Dlk1-Gtl2 locus suggests their involvement in expression of paternally expressed genes in mice. *J Reprod Dev* **63**, 101-109 (2017).
41. S. Quenneville *et al.*, In embryonic stem cells, ZFP57/KAP1 recognize a methylated hexanucleotide to affect chromatin and DNA methylation of imprinting control regions. *Mol Cell* **44**, 361-372 (2011).

42. R. Strogantsev, A. C. Ferguson-Smith, Proteins involved in establishment and maintenance of imprinted methylation marks. *Brief Funct Genomics* **11**, 227-239 (2012).
43. H. L. Kenerson, S. Subramanian, R. McIntyre, M. Kazami, R. S. Yeung, Livers with constitutive mTORC1 activity resist steatosis independent of feedback suppression of Akt. *PLoS One* **10**, e0117000 (2015).
44. H. L. Kenerson *et al.*, Akt and mTORC1 have different roles during liver tumorigenesis in mice. *Gastroenterology* **144**, 1055-1065 (2013).
45. S. Labialle *et al.*, The miR-379/miR-410 cluster at the imprinted Dlk1-Dio3 domain controls neonatal metabolic adaptation. *EMBO J* **33**, 2216-2230 (2014).
46. I. Sanli *et al.*, Meg3 Non-coding RNA Expression Controls Imprinting by Preventing Transcriptional Upregulation in cis. *Cell Rep* **23**, 337-348 (2018).
47. N. Takahashi *et al.*, Deletion of Gtl2, imprinted non-coding RNA, with its differentially methylated region induces lethal parent-origin-dependent defects in mice. *Hum Mol Genet* **18**, 1879-1888 (2009).
48. W. Zhu *et al.*, Meg3-DMR, not the Meg3 gene, regulates imprinting of the Dlk1-Dio3 locus. *Dev Biol* 10.1016/j.ydbio.2019.07.005 (2019).
49. P. P. Hsu *et al.*, The mTOR-regulated phosphoproteome reveals a mechanism of mTORC1-mediated inhibition of growth factor signaling. *Science* **332**, 1317-1322 (2011).
50. A. M. Robitaille *et al.*, Quantitative phosphoproteomics reveal mTORC1 activates de novo pyrimidine synthesis. *Science* **339**, 1320-1323 (2013).
51. Y. Yu *et al.*, Phosphoproteomic analysis identifies Grb10 as an mTORC1 substrate that negatively regulates insulin signaling. *Science* **332**, 1322-1326 (2011).
52. Z. Luo *et al.*, Regulation of the imprinted Dlk1-Dio3 locus by allele-specific enhancer activity. *Genes Dev* **30**, 92-101 (2016).
53. Y. Stelzer, I. Sagi, O. Yanuka, R. Eiges, N. Benvenisty, The noncoding RNA IPW regulates the imprinted DLK1-DIO3 locus in an induced pluripotent stem cell model of Prader-Willi syndrome. *Nat Genet* **46**, 551-557 (2014).
54. Y. Wang *et al.*, A permissive chromatin state regulated by ZFP281-AFF3 in controlling the imprinted Meg3 polycistron. *Nucleic Acids Res* **45**, 1177-1185 (2017).
55. X. Xu *et al.*, Dppa3 expression is critical for generation of fully reprogrammed iPS cells and maintenance of Dlk1-Dio3 imprinting. *Nat Commun* **6**, 6008 (2015).
56. V. T. Samuel *et al.*, Fasting hyperglycemia is not associated with increased expression of PEPCK or G6Pc in patients with Type 2 Diabetes. *P Natl Acad Sci USA* **106**, 12121-12126 (2009).
57. R. W. Hunter *et al.*, Metformin reduces liver glucose production by inhibition of fructose-1-6-bisphosphatase. *Nature Medicine* **24**, 1395-+ (2018).
58. A. K. Madiraju *et al.*, Metformin suppresses gluconeogenesis by inhibiting mitochondrial glycerophosphate dehydrogenase. *Nature* **510**, 542-+ (2014).
59. R. A. Miller *et al.*, Biguanides suppress hepatic glucagon signalling by decreasing production of cyclic AMP. *Nature* **494**, 256-260 (2013).
60. Y. Ioannides, K. Lokulo-Sodipe, D. J. Mackay, J. H. Davies, I. K. Temple, Temple syndrome: improving the recognition of an underdiagnosed chromosome 14 imprinting disorder: an analysis of 51 published cases. *J Med Genet* **51**, 495-501 (2014).

61. M. Kagami *et al.*, Temple syndrome: comprehensive molecular and clinical findings in 32 Japanese patients. *Genet Med* **19**, 1356-1366 (2017).
62. R. Gumienny *et al.*, High-throughput identification of C/D box snoRNA targets with CLIP and RiboMeth-seq. *Nucleic Acids Res* **45**, 2341-2353 (2017).
63. M. Khorshid, C. Rodak, M. Zavolan, CLIPZ: a database and analysis environment for experimentally determined binding sites of RNA-binding proteins. *Nucleic Acids Res* **39**, D245-252 (2011).
64. S. Anders, W. Huber, Differential expression analysis for sequence count data. *Genome Biol* **11**, R106 (2010).
65. M. Cornu *et al.*, Hepatic mTORC1 controls locomotor activity, body temperature, and lipid metabolism through FGF21. *Proc Natl Acad Sci U S A* **111**, 11592-11599 (2014).
66. T. K. Wojdacz, L. L. Hansen, A. Dobrovic, A new approach to primer design for the control of PCR bias in methylation studies. *BMC Res Notes* **1**, 54 (2008).
67. M. E. Ritchie *et al.*, limma powers differential expression analyses for RNA-sequencing and microarray studies. *Nucleic Acids Res* **43**, e47 (2015).

Figure Legends:

Fig. 1: *Dlk1-Dio3* locus non-coding genes are up-regulated in L-Tsc1KO mouse livers.
A) miRNA landscape in L-Tsc1KO mice shown as log2 fold change over Control levels. Black dots represent miRNAs that are statistically different (adj.p<0.05) between L-Tsc1KO and Control mouse livers.
B) qPCR validation of a few significantly changing miRNAs. U6 snoRNA is used as a control.
C) Levels of three lncRNAs, *Meg3*, *Rian* and *Mirg*, as well as the protein-coding genes of the *Dlk1-Dio3* locus measured by qPCR shown as fold change to Control.
D) Levels of other non-coding genes found at the *Dlk1-Dio3* locus, ICR-ncRNA (a non-coding transcript associated with increased transcription), snoRNA-MBII-343 and two pre-miRNAs (pre-miR-127 and pre-miR-541), shown as fold change over Control.

Fig. 2: Sustained mTOR signaling up-regulates expression of *Dlk1-Dio3* locus non-coding genes in 8-week-old L-Tsc1KO mice.
A) qPCR showing miRNA levels of 4 and 8-week-old livers from Control or L-Tsc1KO mice. Values are shown as fold change to the control 4-week-old livers.
B) qPCR showing mature miRNA levels in C57BL/6J (wild type) mice at 4 and 8 weeks of age. Values are shown relative to 4-week-old values.
C) qPCR showing mature miRNA levels upon treatment with vehicle or rapamycin (Rapa bars). Values are shown as fold change comparisons of L-Tsc1KO (Vehicle treated) and L-Tsc1KO Rapa (Rapamycin treated) to Control mice (Vehicle treated). To assess significance L-Tsc1KO values are compared to Control values and L-Tsc1KO Rapa values are compared to L-Tsc1KO values.
D) qPCR showing mature miRNA levels upon treatment with vehicle or INK128 (INK128 bars). Values are shown as fold change comparisons of L-Tsc1KO (Vehicle treated), L-Tsc1KO INK128 (INK128 treated) and Control INK128 (INK128 treated) to Control mice (Vehicle treated). To assess significance L-Tsc1KO values are compared to Control values and L-Tsc1KO INK128 values are compared to L-Tsc1KO values.
E) qPCR showing *Meg3*, *Rian* and *Mirg* levels of 4 and 8-week-old mouse livers from Control or L-Tsc1KO mice. Values are shown as fold change to the Control 4-week mouse livers.
F) qPCR showing *Meg3*, *Rian* and *Mirg* levels upon treatment with vehicle or rapamycin (Rapa bars). Values are shown as fold change comparisons of L-Tsc1KO (Vehicle treated) and L-Tsc1KO Rapa (Rapamycin treated) to Control mice (Vehicle treated). To assess significance L-Tsc1KO values are compared to Control values and L-Tsc1KO Rapa values are compared to L-Tsc1KO values.
G) qPCR showing *Meg3*, *Rian* and *Mirg* levels upon treatment with vehicle or INK128 (INK128 bars). Values are shown as fold change comparisons of L-Tsc1KO (Vehicle treated), L-Tsc1KO INK128 (INK128 treated) and Control INK128 (INK128 treated) to Control mice

(Vehicle treated). To assess significance L-Tsc1KO values are compared to Control values and L-Tsc1KO INK128 values are compared to L-Tsc1KO values.

Fig 3: CpG methylation and histone occupancy is reduced in L-Tsc1KO livers at 8 weeks of age.
A) CpG methylation, measured via bisulfite pyrosequencing, at IG-DMR and MEG-DMR in 4-week and 8-week livers of Control and L-Tsc1KO mice. Values are shown as log2 fold change over 4-week-old liver samples of the respective genotype. The median and the range in CpG methylation is shown for each sample. Nlme R-package is used to determine significance.
B) Percent methylation measured at IG-DMR and MEG-DMR for 4 and 8-week-old wild type mice.
C) Percent methylation measured at IG-DMR and MEG-DMR for 4-week-old Control and L-Tsc1KO mice.
D) Percent methylation measured at IG-DMR and MEG-DMR for 8-week-old Control and L-Tsc1KO mice.
E) Percent CpG methylation measured at IG-DMR and MEG-DMR via restriction assay using livers from 8-week-old Control and L-Tsc1KO mice that were treated with vehicle or Rapamycin (Rapa labeled) for 4 weeks from 4 weeks of age. To assess significance L-Tsc1KO values are compared to Control values and L-Tsc1KO Rapa values are compared to L-Tsc1KO values.
F) Percent CpG methylation measured at IG-DMR and MEG-DMR via restriction assay using livers from 8-week-old Control and L-Tsc1KO mice that were treated with vehicle or INK128 (INK128 labeled) for 4 weeks from 4 weeks of age. To assess significance L-Tsc1KO values are compared to Control values and L-Tsc1KO INK128 values are compared to L-Tsc1KO values.
G) CpG methylation, measured via bisulfite pyrosequencing, at MEG-DMR in 8-week-old Control and L-Tsc1KO mouse livers treated with vehicle or INK128 for 4 weeks starting at 4-weeks of age. Values are shown as log2 fold change difference of L-Tsc1KO mouse livers, either vehicle or INK128 treated, over control mouse livers of the same treatment. The median and the range in CpG methylation is shown for each sample. Nlme R-package is used to determine significance.
H) Percent CpG methylation measured at the MEG-DMR using livers from 14-week-old Control and L-Tsc1KO mice.
I) ChIP assay showing occupancy of KAP1 and SETDB1 at MEG-DMR regions of Control and L-Tsc1KO mice. Data are shown as fold change compared to occupancy of respective Control samples.
J) ChIP assay showing occupancy of H2A, H3 and H4 histone proteins at MEG-DMR regions of Control and L-Tsc1KO mice. Data are shown as percent of the input.

Fig 4: *Dlk1-Dio3* locus miRNAs play a role in gluconeogenesis and glucose metabolism.

In this figure at least 4 male mice of 14 to 16 weeks of age were used per condition.
A) Glucose Tolerance Test (GTT) of Control and L-Tsc1KO mice. Area under the curve (AUC) is shown to right to determine significance.
B) Pyruvate Tolerance Test (PTT) of Control and L-Tsc1KO mice. Area under the curve (AUC) is shown to right to determine significance.
C) Glucose Tolerance Test (GTT) of L-Tsc1KO versus L-Tsc1KO miRKO mice. Area under the curve (AUC) is shown to right of each graph to determine significance.
D) Pyruvate Tolerance Test (PTT) of L-Tsc1KO versus L-Tsc1KO miRKO mice. Area under the curve (AUC) is shown to right to determine significance.
E) qPCR showing transcript levels of enzymes involved in the gluconeogenesis pathway. The comparison between L-Tsc1KO mice to Control mice is shown.
F) qPCR showing transcript levels of enzymes involved in the gluconeogenesis pathway. The comparison between L-Tsc1KO miRKO mice to L-Tsc1KO mice is shown.
G) Blood glucose levels measured after 18 hours of starvation. The comparison of L-Tsc1KO mice to Control mice is shown.
H) Blood glucose levels measured after 18 hours of starvation. The comparison between L-Tsc1KO miRKO and L-Tsc1KO mice is shown.

Fig 5: Loss of TSC1 regulates *Dlk1-Dio3* locus miRNAs to affect gluconeogenesis.
Changes with regard to *Dlk1-Dio3* locus miRNAs are depicted in 4-week versus 8-week-old animals in Control and L-Tsc1KO mice. CpG islands at IG-DMR and MEG DMR are shown with filled (methylated) or empty (unmethylated) circles, miRNAs are shown with vertical lines.

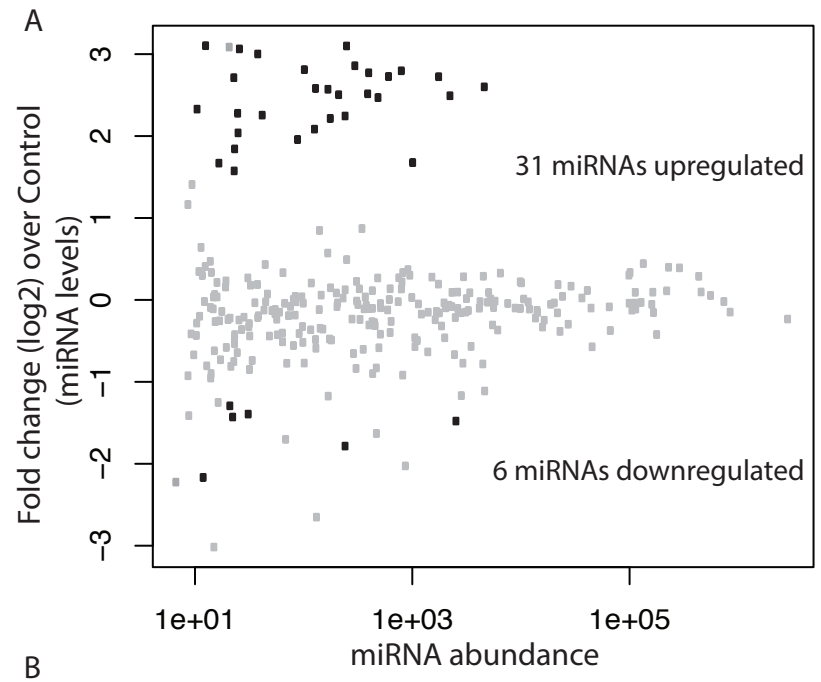
A
Fold change (log2) over Control
(miRNA levels)
3
2
1
0
−1
−2
−3
31 miRNAs upregulated
6 miRNAs downregulated
1e+01
1e+03
1e+05
miRNA abundance

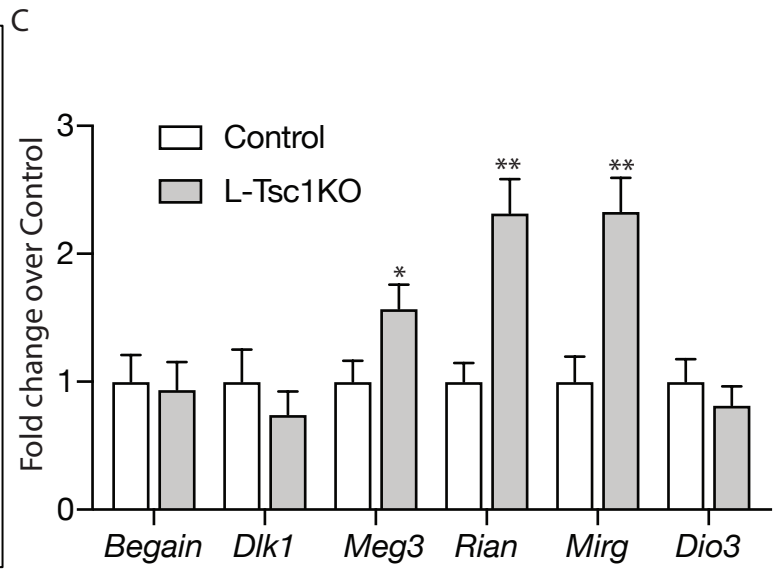
C
Fold change over Control
3
2
1
0
Control
L-Tsc1KO
*
**
**
Begain
Dlk1
Meg3
Rian
Mirg
Dio3

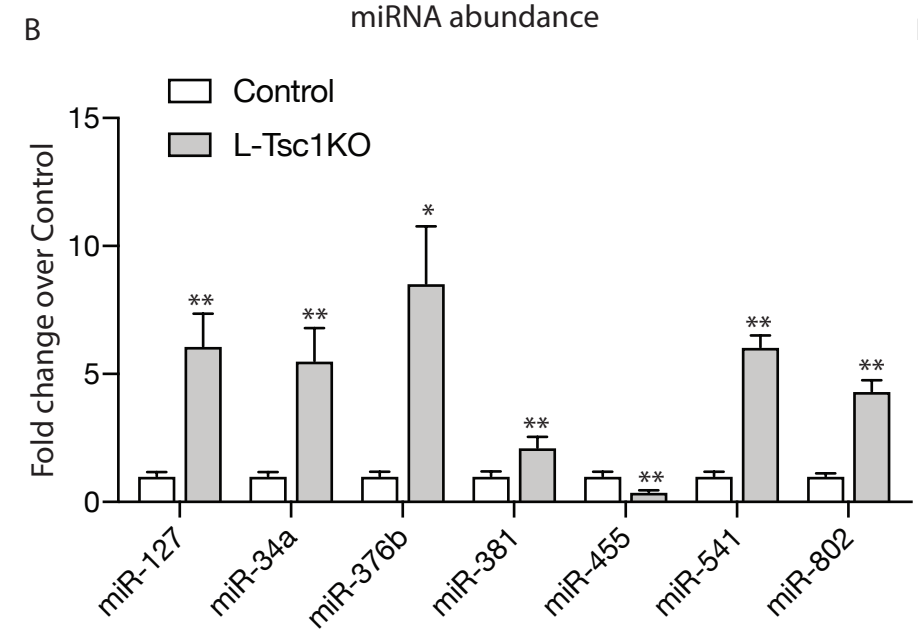
B
Fold change over Control
15
10
5
0
Control
L-Tsc1KO
**
**
*
**
**
**
**
miR-127
miR-34a
miR-376b
miR-381
miR-455
miR-541
miR-802

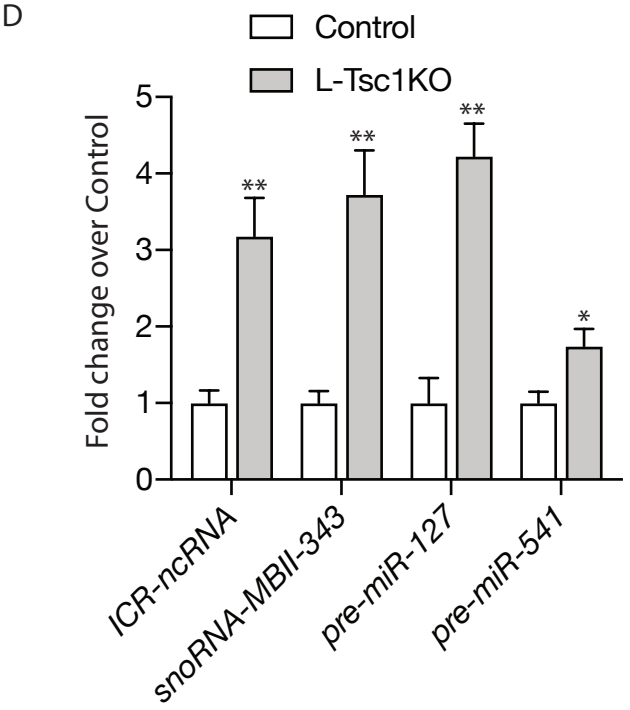
D
Fold change over Control
5
4
3
2
1
0
Control
L-Tsc1KO
**
**
**
*
ICR-ncRNA
snoRNA-MBII-343
pre-miR-127
pre-miR-541

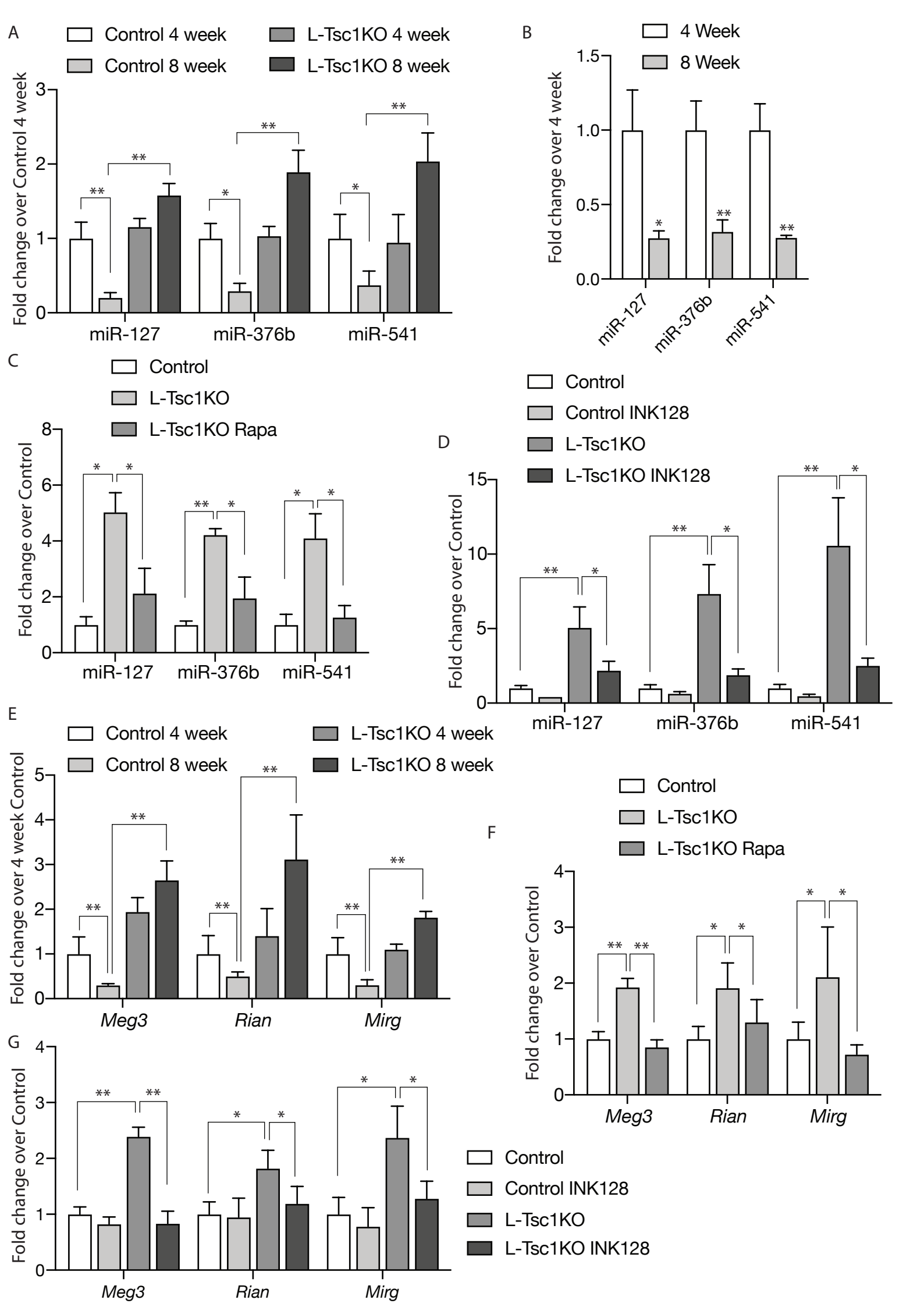
A
Control 4 week
Control 8 week
L-Tsc1KO 4 week
L-Tsc1KO 8 week
Fold change over Control 4 week
miR-127
miR-376b
miR-541
B
4 Week
8 Week
Fold change over 4 week
miR-127
miR-376b
miR-541
C
Control
L-Tsc1KO
L-Tsc1KO Rapa
Fold change over Control
miR-127
miR-376b
miR-541
D
Control
Control INK128
L-Tsc1KO
L-Tsc1KO INK128
Fold change over Control
miR-127
miR-376b
miR-541
E
Control 4 week
Control 8 week
L-Tsc1KO 4 week
L-Tsc1KO 8 week
Fold change over 4 week Control
Meg3
Rian
Mirg
F
Control
L-Tsc1KO
L-Tsc1KO Rapa
Fold change over Control
Meg3
Rian
Mirg
G
Fold change over Control
Meg3
Rian
Mirg
Control
Control INK128
L-Tsc1KO
L-Tsc1KO INK128

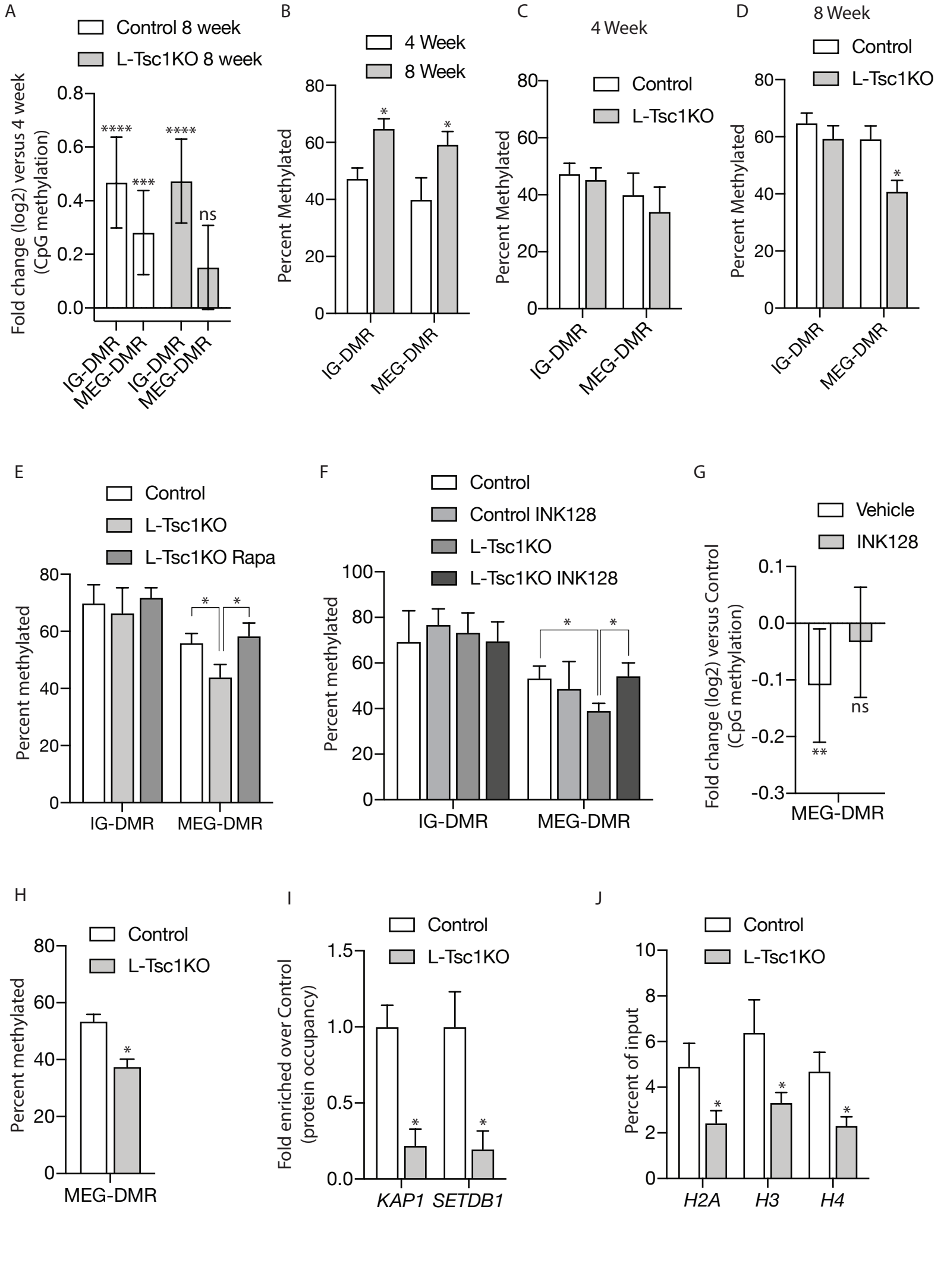
A
Control 8 week
L-Tsc1KO 8 week
Fold change (log2) versus 4 week (CpG methylation)
0.8
0.6
0.4
0.2
0.0
****
***
****
ns
IG-DMR
MEG-DMR
IG-DMR
MEG-DMR
B
4 Week
8 Week
Percent Methylated
80
60
40
20
0
*
*
IG-DMR
MEG-DMR
C
4 Week
Control
L-Tsc1KO
Percent Methylated
80
60
40
20
0
IG-DMR
MEG-DMR
D
8 Week
Control
L-Tsc1KO
Percent Methylated
80
60
40
20
0
*
IG-DMR
MEG-DMR
E
Control
L-Tsc1KO
L-Tsc1KO Rapa
Percent methylated
80
60
40
20
0
* *
IG-DMR
MEG-DMR
F
Control
Control INK128
L-Tsc1KO
L-Tsc1KO INK128
Percent methylated
100
80
60
40
20
0
* *
IG-DMR
MEG-DMR
G
Vehicle
INK128
Fold change (log2) versus Control (CpG methylation)
0.1
0.0
-0.1
-0.2
-0.3
**
ns
MEG-DMR
H
Control
L-Tsc1KO
Percent methylated
80
60
40
20
0
*
MEG-DMR
I
Control
L-Tsc1KO
Fold enriched over Control (protein occupancy)
1.5
1.0
0.5
0.0
* *
KAP1
SETDB1
J
Control
L-Tsc1KO
Percent of input
10
8
6
4
2
0
* * *
H2A
H3
H4

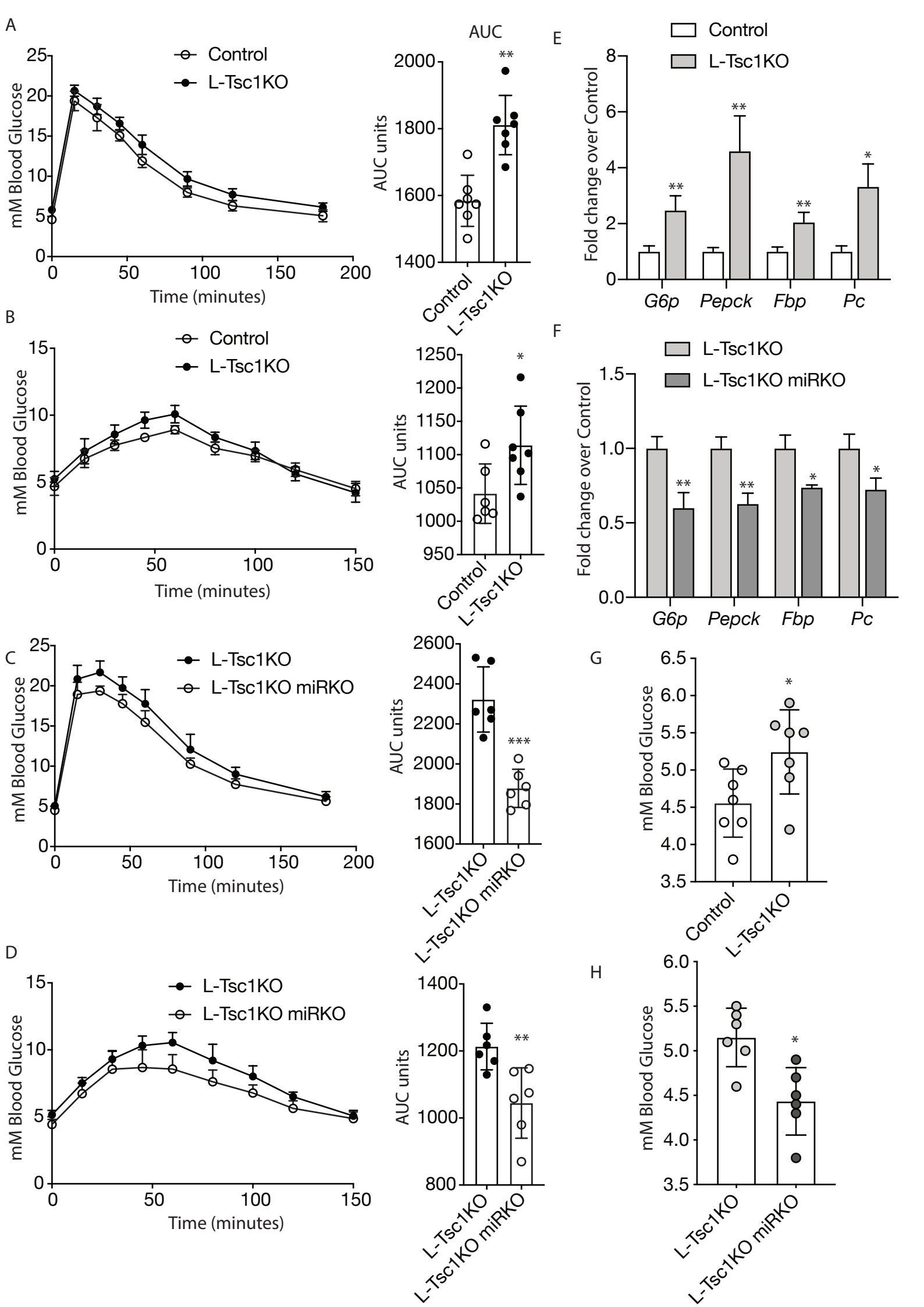
A
Control
L-Tsc1KO
mM Blood Glucose
Time (minutes)
AUC
AUC units
Control
L-Tsc1KO
B
Control
L-Tsc1KO
mM Blood Glucose
Time (minutes)
AUC units
Control
L-Tsc1KO
C
L-Tsc1KO
L-Tsc1KO miRKO
mM Blood Glucose
Time (minutes)
AUC units
L-Tsc1KO
L-Tsc1KO miRKO
D
L-Tsc1KO
L-Tsc1KO miRKO
mM Blood Glucose
Time (minutes)
AUC units
L-Tsc1KO
L-Tsc1KO miRKO
E
Control
L-Tsc1KO
Fold change over Control
G6p
Pepck
Fbp
Pc
F
L-Tsc1KO
L-Tsc1KO miRKO
Fold change over Control
G6p
Pepck
Fbp
Pc
G
mM Blood Glucose
Control
L-Tsc1KO
H
mM Blood Glucose
L-Tsc1KO
L-Tsc1KO miRKO

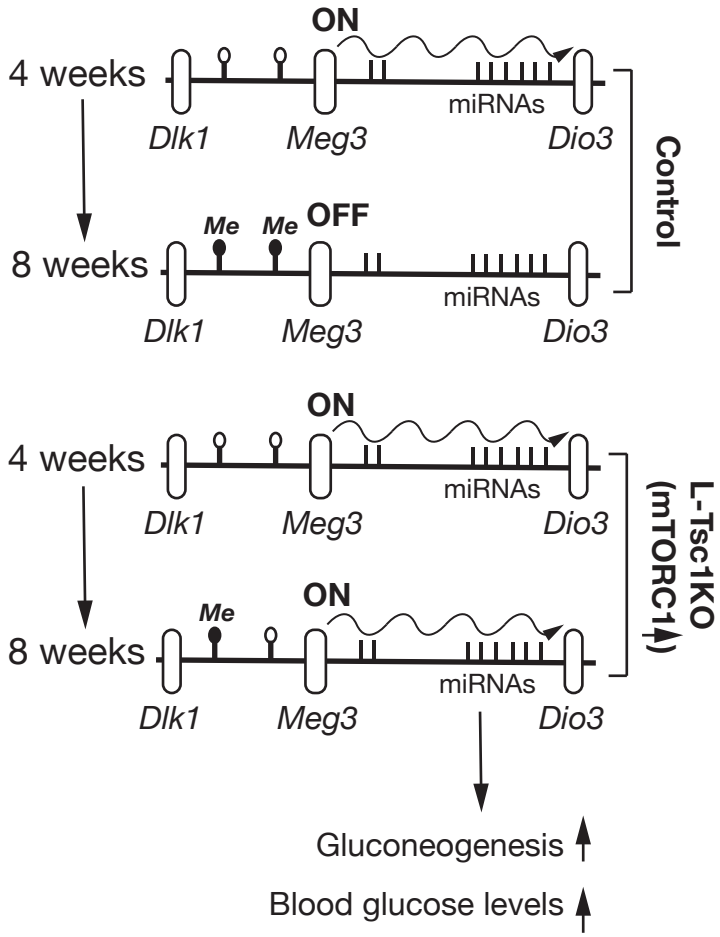
ON
4 weeks
miRNAs
Dlk1
Meg3
Dio3
Control
Me
Me
OFF
8 weeks
miRNAs
Dlk1
Meg3
Dio3
ON
4 weeks
miRNAs
Dlk1
Meg3
Dio3
L-Tsc1KO
(mTORC1↓)
Me
ON
8 weeks
miRNAs
Dlk1
Meg3
Dio3
Gluconeogenesis ↑
Blood glucose levels ↑